ELSEVIER

Ecological and agricultural applications of synchrotron IR microscopy

T.K. Raab [a,*], J.P. Vogel [b]

[a] *Department of Plant Biology, Carnegie Institution of Washington, Stanford, CA 94305, USA*
[b] *US Department of Agriculture, Western Regional Research Center, Albany, CA 94720, USA*

Available online 11 March 2004

Abstract

The diffraction-limited spot size of synchrotron-based IR microscopes provides cell-specific, spectrochemical imaging of cleared leaf, stem and root tissues of the model genetic organism *Arabidopsis thaliana*, and mutant plants created either by T-DNA insertional inactivation or chemical mutagenesis. Spectra in the wavelength region from 6 to 12 μm provide chemical and physical information on the cell wall polysaccharides of mutants lacking particular biosynthetic enzymes ("Cellulose synthase-like" genes). In parallel experiments, synchrotron IR microscopy delineates the role of *Arabidopsis* cell wall enzymes as susceptibility factors to the fungus *Erysiphe cichoracearum*, a causative agent of powdery mildew disease. Three genes, *pmr4*, *pmr5*, and *pmr6* have been characterized by these methods, and biochemical relations between two of the genes suggested by IR spectroscopy and multivariate statistical techniques could not have been inferred through classical molecular biology. In ecological experiments, live plants can also be imaged in small microcosms with mid-IR transmitting ZnSe windows. Small exudate molecules may be spatially mapped in relation to root architecture at diffraction-limited resolution, and the effect of microbial symbioses on the quantity and quality of exudates inferred. Synchrotron IR microscopy provides a useful adjunct to molecular biological methods and underground observatories in the ongoing assessment of the role of root–soil–microbe communication.
© 2004 Elsevier B.V. All rights reserved.

Keywords: Cell wall; Plant pathogen; Rhizosphere; Infrared; Spectromicroscopy

1. Genetic dissection of plant cell walls

Given the limited mobility of plants, a variety of carbon- and nitrogen-based polymers must be articulated to provide structural rigidity and defense from pathogens, while at the same time allowing both the shoot and root system to proliferate when environmental conditions and resources are optimum. Cellulose, an abundant, crystalline β-1,4-linked glucose polymer, is a major source of fiber. Several large classes of plant-derived carbohydrate polymers are less well known [1,2]. Xylan is the predominant non-crystalline polysaccharide of hardwoods and agricultural crops, and is a β-linked polymer of xylose. It occurs in the hemicellulose fraction of plant cell walls, and is responsible for the swelling properties

* Corresponding author. Tel.: +1-650-325-1521x446; fax: +1-650-325-6857.
E-mail address: tkraab@andrew2.stanford.edu (T.K. Raab).

and biodegradation characteristics of woody biomass [3,6]. Cellulose and xylan share a high degree of macromolecular organization when deposited in cell walls. In contrast, a third family of polysaccharides, the pectins, form an amorphous "gel" between cellulose and xylans, and are comprised of highly acidic uronic acids with a great diversity of sugar linkages. While enzymes catalyzing the biosynthesis of cellulose in both bacteria and plants have been cloned and characterized [4,7], the situation for other carbohydrate polymers in cell walls is not so advanced. Any spectrochemical technique which can provide a synoptic snapshot of the relative abundance of these polymer classes would greatly facilitate our understanding of their structure and function.

A few years ago, the Carnegie Lab [5] started a research effort to understand more about the construction of the cell walls of plants using a "reverse genetics" approach. Based on the published sequence data for cellulose synthases, protein prediction software searched the *Arabidopsis* genome for similar enzymes. Thirty divergent sequences were found, though apparently they do not code for enzymes synthesizing cellulose, but presumably the other polymers comprising the cell wall (they are now known as "Cellulose Synthase-like" genes). The enzymes show sequence similarity to family 2 of processive β-glycosyltransferases [7]. A phylogenetic tree created in the lab of Malcolm Brown (www.botany.utexas.edu/cen/library/tree/default.html) is shown in Fig. 1, and has both the CesAs (the true cellulose synthases) as well as the CsLs. Using either T-DNA or transposon insertional inactivation, we have created homozygous "knockout" lines in 17 of the genes shown in the CsL Family Tree. The research strategy has been to examine by synchrotron IR microscopy cleared samples of leaf, stem or root tissue in mutant and wildtype *Arabidopsis* plants grown under carefully controlled environmental conditions. The very tight, compact beam size of the synchrotron at ALS Beamline 1.4.3. allows us to interrogate specific cell types [8]. Using a con-
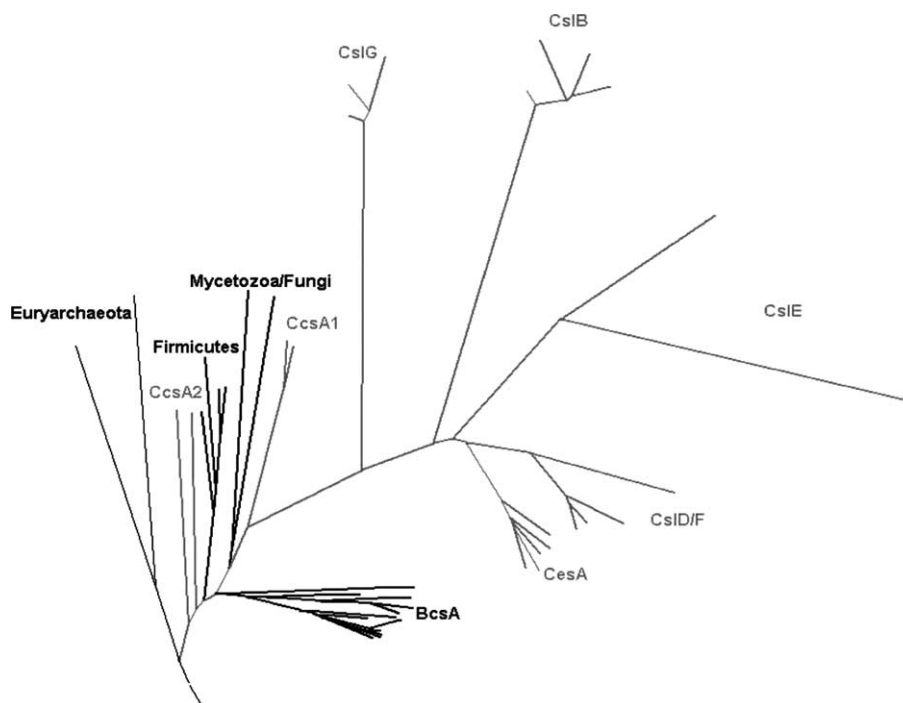

Fig. 1. Unrooted phylogentic tree of the cellulose synthase superfamily for bacteria, algae, fungi and higher plants, and the "cellulose synthase-like" (Csl) genes of plants.

ventional IR source in some experiments leads to an averaging over many cell types [9,10]. Multivariate statistical methods such as 'principal components analysis' are used to detect differences, and an approximate molecular identification of the lesion made. Further wet-chemistry methods are brought to bear to determine the nature of the cell wall polymer synthesized by the missing gene [2,11]. For the analytical side of our work, we utilize GC-MS and capillary electrophoresis to determine the sugar composition and specific linkages within fractions from the cell wall. Other groups are now trying to apply a similar strategy to rice, the next plant for which complete genomic sequence will become available [12]. The mid-infrared spectral comparison (Fig. 2) shows one of the products from IR analysis of cell walls. In this case we identify a good mutant candidate among the "B" family of CsLs that may be missing an enzyme responsible for synthesizing xyloglucans, major load-bearing polymers in plant cell walls [13].
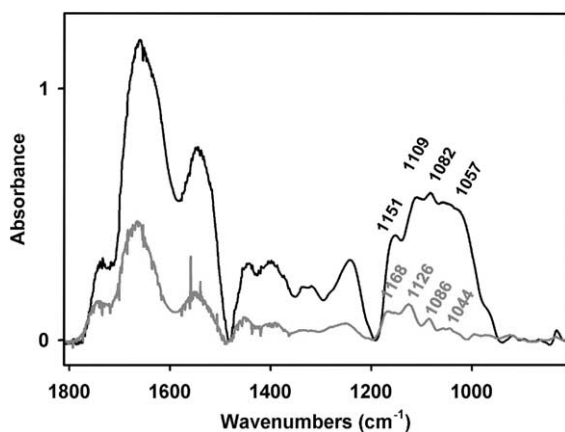

Fig. 2. Comparison of leaf IR spectra from *Arabidopsis* mutants lacking the *CsLB6* gene (dark curve), and *Col-0* wild type plants (light curve). Each curve represents the mean of 10 plants. Note in the region 1200–1000 cm^{-1}, shifts in relative intensity and peak energy for several peaks. *Col-0* peak assignments: 1168 cm^{-1} xyloglucan v(CC), v(CO), v(COC) [23]; 1126 cm^{-1} cellulose v(CO), v(CC) [13]; 1086 cm^{-1} cellulose [25]; 1044 cm^{-1} pectate CO ring [28]. *CsLB6-1* peak assignments: 1151 cm^{-1} cellulose ring w/extra H-bonding [25], 1109 cm^{-1} uronic acids [27]; 1082 cm^{-1} cellulose w/H-bonding shift [25]; 1057 cm^{-1} pectin v(CO), v(CC), δ(OCH) [13]. Numbers in square brackets refer to literature cited in this paper.

2. Plant disease susceptibility factors

Understanding the molecular basis of plant resistance to disease contributes to reducing worldwide crop losses. Over 6000 plant species are infected by powdery mildew, and losses worldwide from plant disease outbreaks may exceed $1 billion each year. Our model organism for studying disease resistance is *Arabidopsis thaliana*, a small member of the mustard family for which complete genomic sequence information [14] was publicly released in 2000. Using *Arabidopsis* as a model genetic organism infected by *Erysiphe cichoracearum* (the causative fungal agent of powdery mildew), we hope to be able to rapidly identify and transfer genes for disease resistance.

Erysiphe cichoracearum colonizes and eventually overtakes a host if three events occur. *Erysiphe* spores are carried on the wind, and when they land on the aerial portions of a host plant (Fig. 3), they must invade an epidermal (outer) cell, and establish a feeding structure to divert plant nutrients [15]. The fungus must "fly under the radar" of the host's defense responses, which would, if fully activated, quickly kill the invading fungus. Since the fungus is an obligate biotroph and not a saprophytic pathogen (i.e., it cannot survive on dead tissues), it must keep the plant host alive until its own life cycle is complete. Several genetic loci conferring *powdery mildew resistance (pmr1*
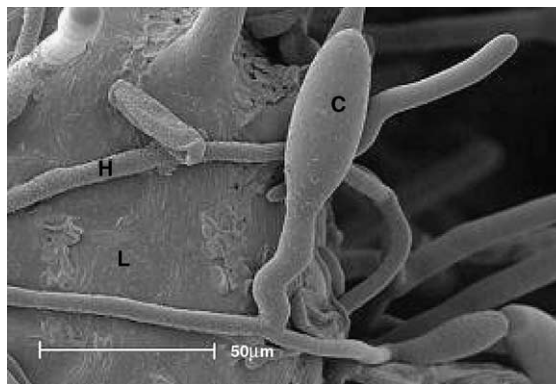

Fig. 3. Scanning electron microscope photo of an *Erysiphe* spp. fungus (causative agent of powdery mildew) growing on the surface of a leaf (L) with both reproductive conidiophores (C) and hyphal feeding (H) structures visible. Scale bar is 50 μm.

through *pmr4*) were previously identified by Vogel and Somerville [16]. While many disease-resistance pathways involve sensing of salicylic acid or ethylene-jasmonic acid, several genes that operate independently of these hypersensitive responses have been identified. We now describe in more detail two mutants representing novel forms of disease resistance based upon loss of a gene required during a compatible interaction, rather than the action of known host defense pathways.

The most curious gene uncovered in the forward genetic screen for powdery mildew resistance was *PMR6*. Cloning demonstrated that the gene was a pectate lyase-like enzyme with a novel carboxy-terminal extension [17], and a member of a seemingly large gene family in *Arabidopsis*. This enzyme cleaves α-1,6-linked polygalacturonic acid chains within pectins, and is presumably used by the plant to reconfigure the cell wall during growth. The enzyme serves as a susceptibility factor under pathogen stress. Removal of the enzyme made the plant resistant to the fungus, with no evidence for activation of normal plant defense responses. As mentioned before, our knowledge of the substrates and mechanism of cell wall enzymes is limited to "true" cellulose synthases, so all attempts to demonstrate enzymatic activity in crude preparations of the *PMR6* gene product failed. IR microscopy was utilized previously for identifying global alterations in cell wall composition in plants [9,10], so cleared leaf preparations of the mutants were compared (Fig. 4) by synchrotron IR microscopy to determine if the identification of missing cell wall polymers could be made. Spectral comparison using principal component's analysis for this mutant are described in more detail in Section 3.

PMR5 is the most recently cloned locus in a search for plant genes mediating resistance to fungal pathogens. Characterization and cloning [18] of *PMR5* demonstrated that it codes for a membrane-associated 402 aa-protein, unique to plants and again part of a large gene family, with a coding sequence having very few recognizable protein structural motifs—a true "pioneer" protein. However, the first 22 amino acids of the protein are predicted to serve as an N-terminal secretory sequence for the endoplasmic reticulum.
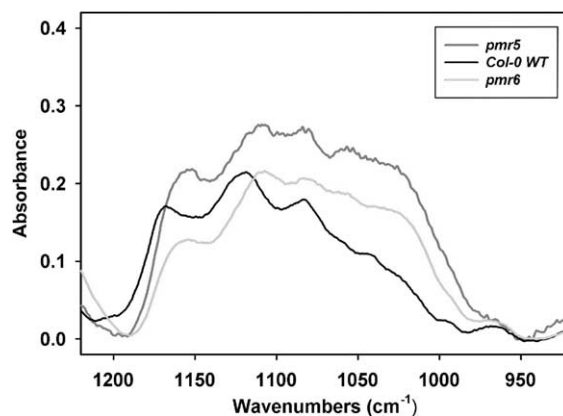

Fig. 4. Comparison of mean *Columbia* wildtype (top) *Arabidopsis* spectra with the *pmr6* (middle) and *pmr5* (bottom) mutants. Notice the high degree of similarity in the region from 1200 to 950 cm^{-1} region for the two mutant lines. The skeletal vibrations of hexose sugar rings, as well as the v(C–O–C) of pyranose rings and glycosidic bonds occur in this region. Each spectrum is the mean of at least a dozen plants. IR band assignments follow the legend in Fig. 2.

Compared to wild type plants, the visual phenotype of *pmr5* mutant plants is similar to the previously described *pmr6* mutation [16], in that the overall size of the plants are reduced, the leaves cup upward, and most importantly have quantitative resistance to powdery mildew fungus. The mutants' novelty arise from neither genotype depending on activation of the salicylic acid (SA)- or jasmonic acid/ethylene-dependent pathways for defense. To provide understanding of the underlying molecular lesion, we undertook at ALS Beamline 1.4.3 an IR spectromicroscopic comparison of leaves from plants homozygous for mutations in either *pmr6* or *pmr* 5, and wildtype plants. We supplemented this IR analysis with direct biochemical extractions of the cell walls from similar plants to those used for the IR studies. The spectra (Fig. 4) from top to bottom are the *pmr5* mutant, the *pmr6* mutant, and the wild type comparison plants. Notice the high degree of similarity in the polysaccharide "fingerprint" IR region of 1200–950 cm^{-1}. This is a remarkable result in that we had no reason (other than the visual similarity of the mutants) to suspect a metabolic connection between the two mutants. Chemical and genetic tests are underway to

uncover whether the two genes operate in the same pathway, or two parallel pathways [18]. This is an indication of the power of synchrotron IR microscopy to assist in the metabolic characterization of mutants.

3. Exploratory IR data analysis in agriculture and ecology

Spectra from an IR microscope (or any Fourier Transform instrument, for that matter) present a significant challenge with regards to data analysis. If you collect over the region from 5 to 20 μm at 2 cm^{-1} resolution, each spectrum represents 750 individual measurements. Unavoidably, you will always end up with $s \gg n$, where s is the number of data points and n is the number of samples. As well, when we compare two IR spectra, differences can be subtle [19]. To address these problems, there exist methods variously referred to as "Multivariate statistics" or "Chemometrics". These mathematical techniques have been developed to first compress large data sets, and then to bring forward possibly hidden features from spectra [20,21].

One of the simplest and widely used methods, PCA (principal components analysis) uncovers the directions of major variation in spectral data through decomposition of the raw data matrix into a linear combination of independently varying factors. One of the aims of PCA is to achieve a "parsimonious description" of a multivariable data set. First we generate a covariance matrix of the spectral data–covariance being the statistical term measuring how two or more features of our data tend to vary together, or "co-vary". Consider feature i and feature j, and let $\{s(1,i), s(2,i), \ldots, s(n,i)\}$ be a set of n spectra as examples of feature i, and $\{s(1,j), s(2,j), \ldots, s(n,j)\}$ the corresponding example spectra for feature j. The covariance of feature i and feature j is

$$\mathbf{C}(i,j) = \{[s(1,i) - m(i)]^*[s(1,j) - m(j)] + \cdots \\ + [s(n,i) - m(i)]^*[s(n,j) - m(j)]\}/(n-1)$$

Here, $m(i)$ is the mean of feature i, and $m(j)$ the mean of feature j. The covariance matrix has some key features that make intuitive sense:

(i) if spectral feature i and feature j tend to increase together, then $\mathbf{C}(i,j) > 0$,
(ii) if feature i tends to decrease while feature j increases, then $\mathbf{C}(i,j) < 0$,
(iii) if feature i and feature j are independent, then $\mathbf{C}(i,j) = 0$.

The other standard representation of principal components in use is the "Correlation Matrix" representation. However, spectroscopic comparisons are easiest with the covariance matrix [20]. Correlation matrices can be useful if only very small contaminants in products are being sought, for example.

When we perform PCA, we have to make a choice as to how many components to retain in the analysis. There is no hard and fast rule – operationally, researchers sum the % contributions from each PC, and then disregard anything beyond 95% cumulative variance. You can make a graph, sometimes called a "screen plot" or "elbow plot", and choose a cutoff where there is a strong inflection. Do we loose any information by discarding the low-variance contributions, or to say it another way, which are the most informative PCs in a particular chemical spectroscopic comparison? [22] Fig. 5 shows PC1 of the covariance matrix reduction of matched *pmr6* mutant and wildtype data sets. Nearly 85% of the variation in the IR spectral signature between the two classes of plants was attributable to some compound(s) described by PC1. If we look at the PC scores they resemble IR spectra. The PC "scores" are centered about the mean line of zero, and peak loadings that are especially positive or negative contribute most to the signature. The energies of the IR spectral features that have the greatest "loading" or contribution are: 1702, 1609, 1426, 1101 and 1018 cm^{-1}. Since plant tissues were cleared of pigments and waxes prior to spectral collection with solvents, and based on the penetration depth of mid-IR radiation in these tissues, these spectral features arise from cell wall polysaccharides and proteins. Previous workers in the field of plant polysaccharide metabolism [23–29] provide fairly good assignments for most of these bands, and we interpret PC1 as indicating an alteration in the amount of pectin polymer in the cell wall (based
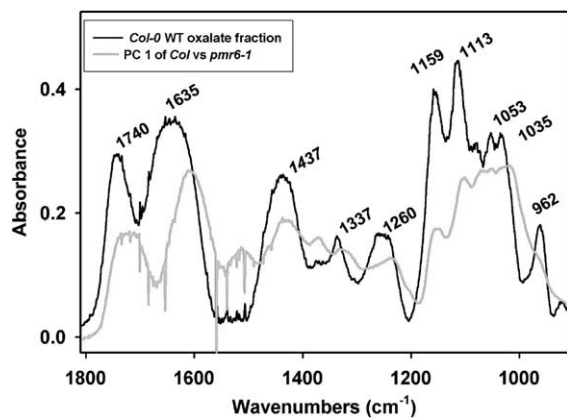
Fig. 5. A comparison of principal component 1 (light spectrum) from the covariance–matrix separation of wildtype *Arabidopsis* from *pmr6* mutants, with a lab spectrum (dark) of ammonium oxalate-extractable pectins. IR band assignments: 1740 cm^{-1} pectin ester v(C=O) [24]; 1635 cm^{-1} pectin adsorbed water δ(HOH) [13]; 1437 cm^{-1} pectin methylester OCH$_2$ deformation [28]; 1337 cm^{-1} δ(CH), ring vibration [13,28]; 1260 cm^{-1} pectin ester COC [28]; 1159 cm^{-1} xylogalacturonan v(CC), v(CO), v(COC) [23]; 1113 cm^{-1} pectin asymmetric in-phase ring [13,23]; 1053 cm^{-1} arabinose-rich pectin [27]; 1035 cm^{-1} polygalacturonic acid [27]; 962 cm^{-1} pectinate carboxyl deformation [28]. Numbers in square brackets refer to literature cited in this paper.

on the absorbances at 1101 and 1018 cm^{-1}), as well as the altered methylesterification of the sugar chains. Cross-correlation with X-ray diffraction data led researchers to suggest that the feature at 1426 cm^{-1} is sensitive to the level of hydrogen-bonding organization of cellulose microfibrils [30]. Overall, the interpretation of the PC1 leads us to a model [17] whereby the mutant's modified pectin composition greatly decreases the "pore size" of the cell wall [31], and is consistent with the biological observation that the fungus grows very slowly, and eventually fails to thrive on *pmr6* mutants plants. The second principal component did not separate the two type of plants, but registers additional peaks (1669 and 1553 cm^{-1}) arising from amide I and II bands of leaf photosynthetic proteins. "Ground truthing", or confirmation of these mathematical loadings from PCA is achieved by sequential chemical extractions from the plant cell wall. For example, we can use Ca^{++}-chelating agents to destabilize the pectin matrix of the cell wall. Fig. 5 is a side-by-side

comparison of Principal Component 1 (lighter color) and purified plant pectin (darker spectrum; extracted with ammonium oxalate). Not a perfect match, but the computational result has quite a bit of similarity to authentic polygalacturonic acid polymers. In the figure legend, we provide the best molecular assignments for these spectra, based on both spectra of purified compounds and normal mode calculations for small model polymers. Polysaccharide spectra are complicated by the presence of both inter- and intra-chain hydrogen bonds connecting the sugars [32]. A very small amount of research on H-bonding networks has been done in the far IR (40–200 μm wavelength) on carbohydrates [33], and as detectors and sources (especially synchrotrons) improve, better spectral assignments will be possible.

4. Ecological applications of synchrotron IR radiation

The belowground life of plants is the part of the biosphere of which we know the least. Early in the last century, ecologists [34,35] traveled desert and grassland ecosystems of North America, painstakingly excavating the (nearly) intact root systems of crops and wild plants. They generated atlases to classify root-growth strategies in different environs that have never really been improved upon or even repeated. These were phenomenal contributions in studying the ecology of plant responses to different climates and soils, but such excavation does not tell us everything about the many varied roles of plant roots. They are not simply structural supports to keep the aboveground parts anchored, nor are they passive straws for the uptake of water and vital nutrients. Roots serve a vital role as a communications network in the soil [36]. During the life of a plant, as much as 15% of the total fixed C will be diverted into sugars, proteins and other small molecules that are 'lost' to the plant in some sense. While these "exudates" preserve the integrity of the soil fabric, they also act as signaling molecules, initiating useful partnerships (symbioses) with microorganisms in the soil. The "textbook" symbiosis between legumes and soil bacteria, principally of the families *Rhizobium* and

Bradyrhizobium, greatly enriches the soil through the incorporation of atmospheric N_2 gas into amino acids for the plant host. In a true case of inter-species cooperation, the plant supplies sugars and other small molecules to support the growth and metabolism of the bacteria. The human importance of this symbiotic relationship cannot be stressed enough – roughly 33% of the dietary protein on the planet comes from legumes. Simply put, researchers would like to speed the adaptation of legumes to growth on marginal soils. Under the warm and moist conditions of the tropics, soil minerals weather much faster than in temperate regions. The mineral surfaces remaining in "acid soils" often retain phosphorus [37], an essential nutrient for plant and animal development, and simultaneously show elevated levels of free $[Al^{3+}]$, an abundant element in soils toxic to root growth when soluble. Plants respond to adverse soil chemistry by increasing the exudation of low-MW organic acids that chelate and effectively decrease the solubility of toxic metals, and releasing specific exoenzymes to enhance absorption of nutrients. Unfortunately, there is virtually no data broadly comparing plant families in their respective exudation strategies towards a particular soil or climatic stress. We now present a brief description of "rhizobox-IR spectromicroscopy" as a way to rationally select plant cultivars for particular soil chemical conditions. In other words, we initially compare spectral identifications of exudates for particular members of a plant family and ask: which set of exudates allows a plant to thrive under a particular soil stress. At the same time we compare the plants' relative efficiency for C-uptake per unit nutrient acquired.

Experimentally, then, how do we integrate a synchrotron infrared source into this type of research? Ecological and agricultural studies have a long history of employing "microcosms" or model systems to study complex processes. Raab and Martin [40] designed small microcosms that they call "rhizoboxes" (Fig. 6). Nearly all common materials like glass and Lexan are essentially opaque in the mid-infrared. What is needed is some relatively tough window material transparent in the mid-IR. Salt windows (e.g. NaCl and KBr) have broad IR transmission, but they fog

Fig. 6. An example of an infrared-transmitting plant microcosm for studying the spatial distribution of root-derived compounds from living plants. The 50 mm × 20 mm zinc selenide window is used for direct imaging with an IR microscope.

easily in moist environments and would eventually dissolve. Many semiconductors (e.g. Ge) transmit IR light over a wide range, though somewhat opaque in the visible, making microscopy difficult. The best choice appears to be zinc selenide (ZnSe), a polycrystalline material with broad IR and visible light transmission (17000 to ∼700 cm^{-1}). The rhizobox windows are 1 mm thick, with an area of 50 mm × 20 mm. An important consideration for biological studies is that ZnSe windows be chemically neutral under all but the most extreme conditions, so as not to react with soil water or roots during experiments.

With small boxes with ZnSe observation windows in the root zone – you can fill them with acid-washed sand, or some other simple substrate for growing plants. Seeds can be germinated directly in the boxes (which are themselves wrapped in Al-foil in the greenhouse to suppress algae growth) and after 2 weeks or so, roots grow past the ZnSe observation window(s). Using the

synchrotron-based IR microscopes at the Advanced Light Source [8], we can collect mid IR spectra in reflectance geometry. This provides a snapshot of the root–soil–water interface zone of an intact plant, and we might choose to simply follow the temporal progression of the exudates from roots during normal growth and development. Previous studies on root anatomy suggested that there is some specialization in both the quantity and quality of exudates released from different parts of the root (reviewed in [36]). Alternatively, we can split our plants into two groups, and subject half of the plants to nutritional stress, heavy metal-toxicity, pathogen attack or climate stress and observe the temporal response of root exudation. The chemical identity of many of the exudates are decipherable from the IR spectra collected, as well as preserving their spatial context. With conventional IR sources, these experiments would not be possible on such a fine spatial scale. Alternatively, if you are interested in what is happening to soil chemistry over time, synchrotron IR spectroscopy has a long and distinguished career in service of mineral chemistry and physics (*see Hemley's contribution, this volume*).

The choice of growth substrate for reflectance spectroscopy of the plants is not entirely random, and it is worth reviewing the logic behind this. We wanted a relatively simple substrate providing good contrast in the mid-IR, and reviewed the remote sensing and planetary astronomy literature for some clues. The cryogenic MCT-A detector in IR microscopes has a small element size and not a very wide "look angle". Unless we have access to a goniometer-like stage for tilting specimens to the incoming synchrotron IR beam, we are limited to the specular reflectance component of a complex soil/water/root interface zone. For any light to actually make it back from the surface to our detector, then, it cannot pass through many complex interfaces (sometimes called "volume scattering") or bounce around the soil. An easy way to do this is to choose a plant growth substrate with average particle size $\sim$5–10$\times$ the interrogating wavelength [41,42]. This is inconvenient for clay chemistry studies, because we are limited to using materials of the silt and size sand classes ($\geqslant$ 53 μm). Much interesting reactivity occurs in clay

mineral size classes ($\sim$2 μm), but clay mineral spacing and the high absorptivity of clay-organic complexes do not provide enough signal for reflectance mode measurements. Soft X-ray beamlines at synchrotrons demonstrate many opportunities for chemical imaging of these important clay and humic materials [43], and may be coupled with IR experiments to build a multi-wavelength picture.

What do you detect in these experiments? Initially we chose the cultivated legume mungbean (*Vigna mungo* L.) and grew two sets of plants, one with complete nutrients, another deprived of phosphorus. If you focus on the plant growth media, you detect IR spectra of silica-feldspathic minerals, as expected. Once you start looking at root surfaces visible through the ZnSe window, you detect protein, lignin, waxes and carbohydrates (Fig. 7A). Next to the spectrum is a visual image captured through the IR microscope of the network of polysaccharides and protein deposited into the soil by plant roots sometimes known as "mucilage" (Fig. 7B). The uronic acid-rich polysaccharides comprising this network are highly charged, absorb large amounts of water [44], ease the passage of roots into soils, stimulate local microbial communities [38,39], mobilize nutrients [45] and improve the structure of soils. Using the very fine focusing of the synchrotron beam, we can directly image these compounds in the rhizoboxes and start to ask evolutionary questions of plant root systems [40,46]. It may be difficult for non-ecologists to appreciate this, but in fact there are very few tools at our disposal to look at the belowground chemistry of intact plant-microbe assemblies. With regards to spatial resolution, synchrotron IR microscopy is equivalent to the best [1]H-magnetic resonance imaging spectroscopy (fMRI) published on plant systems [47], with the advantage that IR spectra will not be degraded in the manner of NMR spectra in the presence of the abundant paramagnetic minerals in terrestrial soils. While soil scientists have developed underground observation systems for roots (rhizotrons), these devices provide little access for chemical analysis of rhizosphere soils. Somewhere in between these various scales of experiments may be found the interdisciplinary approach to studying
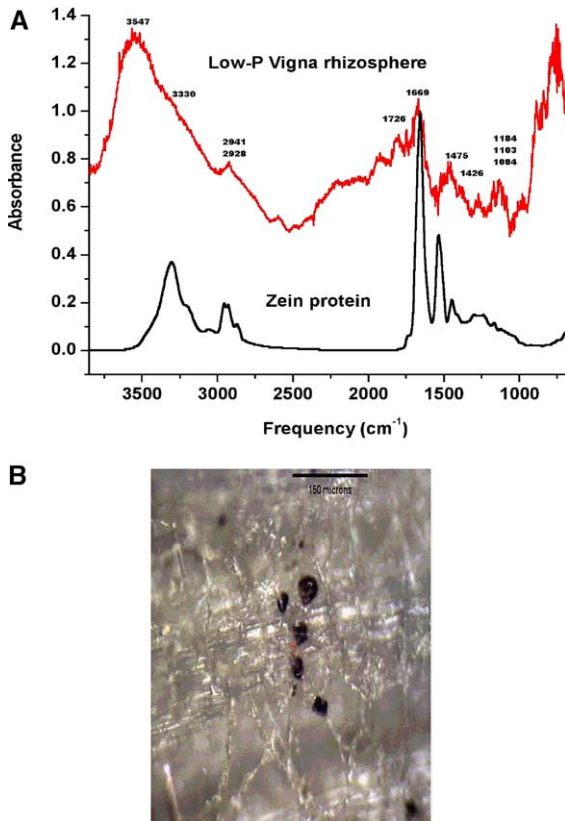
Fig. 7. Comparison (A) of synchrotron IR spectra collected from the rooting zone of the cultivated legume, *Vigna mungo* L. grown under phosphorus-deficient conditions. Purified zein protein presented below for comparison. IR spectral band assignments: 3547 cm^{-1} OH stretch; 3330 cm^{-1} NH stretch for protein; 2941, 2928 cm^{-1} CH$_3$ and CH$_2$ stretches, likely from lipids; 1746 cm^{-1} carbonyl stretch for C$_{16}$–C$_{18}$ fatty acids; 1669 cm^{-1} amide I from protein; 1475 cm^{-1} CH$_2$ scissoring of lipids; 1426 cm^{-1} lipid bending mode; 1184 cm^{-1} ring P–O–C stretching from nucleic acids or polysaccharide; 1103 cm^{-1} arabinogalactan-rich polymers; 1084 cm^{-1} ring mode from xyloglucan. A visual image (B) of the "mucilage" network of *Vigna mungo* roots comprised of highly acidic polygalacturonic acids and protein. Notice the entrained hematite-rich particles. Scale bar is 150 μm.

plants, soils and microbes "in the field". Based on our experience with "rhizoboxes", we argue that broadband synchrotron IR spectroscopy, advanced data-handling techniques (multivariate techniques), or perhaps "machine learning" methods may guide the construction of small, field-portable laser-detector combinations at selected mid-IR wavelengths to detect compounds

relevant to agricultural and ecological research. Such assemblies have a long and distinguished record for gas-phase measurements.

References

[1] T.A. Richmond, C.R. Somerville, Plant Physiol. 124 (2000) 495.
[2] D. Bonetta, M.F. Facette, T.K. Raab, C.R. Somerville, Biochem. Soc. Trans. 30 (2002) 298.
[3] M. Hertzberg, H. Aspeborg, J. Schrader, A. Andersson, R. Erlandsson, K. Blomqvist, R. Bhalerao, M. Uhlen, T.T. Teeri, J. Lundeberg, B. Sundberg, P. Nilsson, G. Sandberg, Proc. Natl. Acad. Sci. USA 98 (2001) 14732.
[4] J.R. Pear, Y. Kawagoe, W.E. Schreckengost, D.P. Delmer, D.M. Stalker, Proc. Natl. Acad. Sci. USA 93 (1996) 12637.
[5] S. Cutler, C.R. Somerville, Curr. Biol. 7 (1997) R108.
[6] S.D. Wullschleger, S. Jansson, G. Taylor, Plant Cell 14 (2002) 2651.
[7] I.M. Saxena, R.M. Brown, M. Fevre, R.A. Geremia, B. Henrissat, J. Bacteriol. 177 (1995) 1419.
[8] M.C. Martin, W.R. McKinney, Proc. Mater. Res. Soc. 524 (1998) 11.
[9] D.L. Wetzel, J.A. Reffner, Cer. Foods World 38 (1993) 9.
[10] L. Chen, N.C. Carpita, W.-D. Reiter, R.H. Wilson, C. Jeffries, M.C. McCann, Plant J. 16 (1998) 385.
[11] T.A. Richmond, C.R. Somerville, Plant Mol. Biol. 47 (2001) 131.
[12] S.P. Hazen, J.S. Scott-Craig, J.D. Walton, Plant Physiol. 128 (2002) 336.

[13] R.H. Wilson, A.C. Smith, M. Kacuráková, P.K. Saunders, N. Wellner, K.W. Waldron, Plant Physiol. 124 (2000) 397.

[14] Arabidopsis Genome Initiative, Nature 408 (2000) 796.

[15] L. Adam, S.C. Somerville, Plant J. 9 (1996) 341.

[16] J.P. Vogel, S.C. Somerville, Proc. Natl. Acad. Sci. USA 97 (2000) 1897.

[17] J.P. Vogel, T.K. Raab, C.L. Schiff, S.C. Somerville, Plant Cell 14 (2002) 2095.

[18] J.P. Vogel, T.K. Raab, S.C. Somerville, Mutations in PMR5 result in powdery mildew resistance and altered cell wall composition, submitted for publication.

[19] M. Defernez, R.H. Wilson, Anal. Chem. 69 (1997) 1288.

[20] E.K. Kemsley, Discriminant Analysis and Class Modeling of Spectroscopic Data, John Wiley and Sons, New York, 1998.

[21] B.S. Everitt, G. Dunn, Applied Multivariate Data Analysis, second ed., Arnold Publishers, London, 2000.

[22] W.J. Krzanowski, P. Jonathan, W.V. McCarthy, M.R. Thomas,, Appl. Stat. 44 (1995) 101.

[23] M. Kacuráková, P. Capek, V. Sainková, N. Wellner, A. Ebringerová, Carbohydr. Polym. 43 (2000) 195.

[24] M.P. Fillipov, J. Appl. Spectr. 17 (1974) 1052.

[25] J.J. Cael, K.H. Gardner, J.L. Koenig, J. Blackwell, J. Chem. Phys. 62 (1975) 1145.

[26] A.S. Barros, I. Mafra, D. Ferreira, S. Cardoso, A. Reis, J.A. Lopes da Silva, I. Delgadillo, D.N. Rutledge, M.A. Coimbra, Carbohydr. Polym. 50 (2002) 85.

[27] M.A. Coimbra, A. Barros, M. Barros, D.N. Rutledge, I. Delgadillo, Carbohydr. Polym. 37 (1998) 241.

[28] N. Wellner, M. Kacuráková, A. Malovikova, R.H. Wilson,, P.S. Belton, Carbohydr. Res. 308 (1998) 123.

[29] G. Mouille, S. Robin, M. Lecomte, S. Pagant, H. Höfte, Plant J. 35 (2003) 393.

[30] Y. Kataoka, T. Kondo, Macromolecules 31 (1998) 760.

[31] S.M. Read, A. Bacic, Cell wall porosity and its determination, in: H.-F. Linskens, J.F. Jackson (Eds.), Modern Methods of Plant Analysis, 17, Springer, Berlin, 1996.

[32] M. Kacuráková, R.H. Wilson, Carbohydr. Polym. 44 (2001) 291.

[33] G.A. Kogan, V.M. Tul'chinsky, M.L. Shulman, S.E. Zurbabyan, A.Y. Khorlin, Carbohydr. Res. 26 (1973) 191.

[34] F.W. Went, Ecology 30 (1949) 1.

[35] J.E. Weaver, Am. J. Bot. 12 (1925) 502.

[36] F.D. Dakora, D.A. Phillips, Plant Soil 245 (2002) 35.

[37] N. Ae, J. Arihara, K. Okada, T. Yoshihara, C. Johnasen, Science 248 (1990) 477.

[38] A.M. Berry, U. Rasmussen, K. Bateman, K. Huss-Danell, S. Lindwall, B. Bergman, New Phytol. 155 (2002) 469.

[39] A.J. van Hengel, K. Roberts, Plant J. 36 (2003) 256.

[40] T.K. Raab, M.C. Martin, Planta 213 (2001) 881.

[41] J.W. Salisbury, J.W. Eastes, Icarus 64 (1985) 586.

[42] M.S. Ramsey, P.R. Christiansen, J. Geophys. Res. 103 (1998) 577.

[43] S.C.B. Myneni, J.T. Brown, G.A. Martinez, W. Meyer-Ilse, Science 286 (1999) 1335.

[44] S.C. Clifford, S.K. Arndt, M. Popp, H.G. Jones, J. Exp. Bot. 53 (2002) 131.

[45] S.A. Welch, W.W. Barker, J.F. Banfield, Geochim. Cosmochim. Acta 63 (1993) 1405.

[46] T.K. Raab, D.A. Lipson, R.K. Monson, Ecology 80 (1999) 2408.

[47] H.H. Rogers, P.A. Bottomley, Agron. J. 79 (1987) 957.